












Protective potential of N-based vaccines against SARS-CoV-2 in a Syrian hamster model

Alexandra Rak^{1,*} , Ekaterina Bazhenova¹ , Polina Prokopenko¹ , Ekaterina Stepanova¹ , Arina Kostromitina¹ , Konstantin Sivak² , Irina Kiseleva¹ , Larisa Rudenko¹  and Irina Isakova-Sivak¹ 

¹Department of Virology and Immunology, Institute of Experimental Medicine, 12 Akademika Pavlova st., 197022 St Petersburg, Russia

²Department of Preclinical Trials, Smorodintsev Research Institute of Influenza, 15/17 Professora Popova st., 197022 St Petersburg, Russia

Abstract:

Introduction: More than 700 million confirmed cases of the novel coronavirus infection COVID-19 have been registered during the 2019-2023 pandemic, and this potentially fatal pathology continues to be identified worldwide. An optimal target for creation of cross-protective vaccines against COVID-19 seems to be the nucleocapsid (N) protein - one of the most conserved and actively produced by infected cells of SARS-CoV-2 antigens. However, the patterns of immune responses induced by N-containing vaccines remain poorly understood. So, the purpose of our study was the comparative investigation of humoral and T-cell immunogenicity of recombinant N protein (rN), N-expressing live attenuated influenza vaccine (LAIV-N), and formalin-inactivated SARS-CoV-2 (SARS-FI) and assessment of the protective effects of these vaccine candidates against homologous SARS-CoV-2 (B.1, Wuhan) strain.

Methods: Syrian hamsters received two injections of experimental vaccines three weeks apart. The effectiveness of the immune responses was measured after 42 days, and protection was tested by exposing the vaccinated hamsters to 10⁵ TCID₅₀ of the challenge virus. To assess intergroup differences, a one-factor ANOVA with Tukey's post-hoc test was used.

Results: A pronounced production of N-specific antibodies and T cells was found following immunization with SARS-FI and rN, whereas only the formation of IFN- γ -synthesizing splenocytes in response to N antigen stimulation was shown for LAIV-N vaccinated animals. Interestingly, LAIV-N and SARS-FI administration significantly prevented virus replication in respiratory organs and progression of infection, while rN vaccination led to better lung tissue performance, but was ineffective for the inhibition of viral airway propagation.

Discussion: Although intraperitoneal injection of recombinant N protein induced robust antibody responses, these effects were insufficient to reduce viral loads in the respiratory tissues of immunized hamsters. At the same time, the N protein delivered by the attenuated influenza vector *via* the intranasal route did not provoke anti-N serum antibodies but stimulated N-specific cellular immune responses and protected animals, partially reducing the viral replication in the upper respiratory tract. This may be explained by the need to engage mucosal or innate immune factors which may be provoked by the LAIV as a carrying vector.

Conclusions: Based on the high immunogenicity and significant protective potential, both inactivated SARS-CoV-2 and modified LAIV encoding the N antigen of SARS-CoV-2 (B.1) demonstrate potential as effective means for protection against COVID-19, in contrast to the recombinant N protein.

Keywords: SARS-CoV-2, COVID-19 vaccine, Syrian hamster, Nucleocapsid protein, Immunogenicity, Cross-protection.

© 2026 The Author(s). Published by Bentham Open.

This is an open access article distributed under the terms of the Creative Commons Attribution 4.0 International Public License (CC-BY 4.0), a copy of which is available at: <https://creativecommons.org/licenses/by/4.0/legalcode>. This license permits unrestricted use, distribution, and reproduction in any medium, provided the original author and source are credited.



Received: October 03, 2025
Revised: November 11, 2025
Accepted: November 25, 2025
Published: March 03, 2026

*Address correspondence to this author at the Department of Virology and Immunology, Institute of Experimental Medicine, 12 Akademika Pavlova st., 197022 St Petersburg, Russia; E-mail: alexandrak.bio@gmail.com

Cite as: Rak A, Bazhenova E, Prokopenko P, Stepanova E, Kostromitina A, Sivak K, Kiseleva I, Rudenko L, Isakova-Sivak I. Protective potential of N-based vaccines against SARS-CoV-2 in a Syrian hamster model. *Open Microbiol J*, 2026; 20: e18742858446108. <http://dx.doi.org/10.2174/0118742858446108251224084746>



Send Orders for Reprints to
reprints@benthamscience.net

1. INTRODUCTION

Although the COVID-19 pandemic, which caused a major socioeconomic crisis, has been officially declared over, new cases continue to emerge globally [1]. The significant mutation rate of the causative agent - SARS-CoV-2 - results in the continuous appearance of novel antigenic variants. This phenomenon compromises both vaccine efficacy and the accuracy of diagnostic tests targeting variable viral antigens, primarily the surface spike protein [2-4]. As a result, spike-targeting immunity alone turns to be insufficient to confer a long-term antiviral protection. A potential solution to the mentioned challenges lies in the use of highly conserved coronavirus antigens as a basis for the development of vaccines and diagnostic tools, for example, the nucleocapsid (N) protein. Quantitatively, it is the major coronavirus antigen that interacts with the viral genome as a homodimer and exhibits active expression in infected cells [5]. The N protein not only provides the genome structuring and protects viral RNA from cellular nucleases, but also, in a histone-like manner, regulates its availability to polymerase and suppresses the host immune responses [6, 7]. The N protein is widely recognized in studies as the most suitable target for stimulating T-cell immune responses [8, 9], whereas to date there are very few data on the functional role and protective properties of abundantly produced N-specific antibodies [10]. Given its pronounced immunogenicity [5, 11] and much higher conservation than that of the traditionally targeted Spike protein [12, 13], the N component appears to be a good alternative antigen for the development of broadly protective COVID-19 vaccines and test systems for the detection of coronavirus or antiviral antibodies [14]. Recent studies of N-containing COVID-19 vaccines developed on various platforms have convincingly demonstrated their immunogenicity, safety, and protective efficacy against infection with both homologous and heterologous viruses [15-18]. It is known, however, that the N antigen is also subjected to evolutionary modifications [19], but their influence on its antigenic properties has been practically unstudied.

Despite the obvious feasibility of targeting the N protein of SARS-CoV-2 for prevention or diagnosis of COVID-19, identification of the optimal vaccine delivery system for N antigen-based formulations remains an unresolved challenge. There are known attempts to develop novel vaccine candidates based on recombinant N

protein in complex with various adjuvants [20-22] or polymeric form [23], as well as on various viral vectors carrying N-coding elements [24-27]. Most of these studies have shown the ability to stimulate specific anti-N immune responses and inhibit replication of challenge viruses to varying degrees in preclinical trials, but undesirable side effects and the need for high doses have been frequently identified.

In this study, we evaluated the immunogenicity and protective efficacy of three prototypes of N-bearing vaccines in a Syrian hamster model. The magnitudes of T- and B-cell immune responses induced by immunization with a vaccine based on recombinant N protein of SARS-CoV-2 variant B.1 (Wuhan), N-bearing live attenuated influenza virus (vectored variant), and formalin-inactivated coronavirus were evaluated, as well as the ability of these prototypes to protect animals from the experimental homologous infection. Based on the previously reported data on the promising potential of triggering N-specific immune responses, at least partial mitigation of disease severity was expected. The choice of the ancestral variant of coronavirus (B.1) for the challenge instead of a more recent and relevant strain was associated with the goal of testing vaccine platforms and determined by the severity of symptoms and the histological picture of lung lesions in experimental animals.

2. MATERIALS AND METHODS

2.1. Cells, Proteins, and Viruses

African green monkey kidney Vero CCL81 cells were acquired from the American Type Culture Collection (ATCC) and maintained in DMEM supplemented with 10% fetal bovine serum (FBS) and 1 × antibiotic-antimycotic (AA) (HiMedia Laboratories Pvt Ltd, Maharashtra, India).

Recombinant N protein of SARS-CoV-2 (B.1), named rN, and NP protein of A/Leningrad/134/17/57 (H2N2) influenza virus were expressed in *E. coli* BL21(DE3) cells as a result of induction with 0.5 mM IPTG and IMAC-purified according to the previously developed protocol [28].

Recombinant RBD protein was expressed in HEK293 cells and sourced from JSC BIOCAD (St Petersburg, Russia).

The source of the SARS-CoV-2 virus HCoV-19/Russia/StPetersburg-3524/2020 (B.1 Lineage, Wuhan) was the Smorodintsev Research Institute of

Influenza (Saint Petersburg, Russia). To measure an infectious titer and propagate the virus at MOI 0.01 as previously described [29] we maintained Vero CCL81 cells at 37 °C and 5% CO₂ in DMEM containing 10 mM HEPES, 2% FBS, and 1 × AA (all from HiMedia Laboratories Pvt Ltd, Maharashtra, India). A complete cytopathic effect was achieved 72 h post-inoculation. The virus-containing media were harvested, clarified *via* gentle centrifugation, divided into aliquots, and stored at -70°C. All procedures involving live SARS-CoV-2 were conducted in a biosafety level 3 (BSL-3) laboratory.

2.2. Modified LAIV Obtaining

A live attenuated influenza virus (LAIV) reassortant bearing the N gene of SARS-CoV-2 (B.1) in the neuraminidase ORF (named LAIV-N) was obtained on the basis of the genome of A/Leningrad/134/17/57 (H2N2) master donor virus (MDV) by plasmid-based reverse genetics. The insertion comprised the full-length N sequence of the ancestral SARS-CoV-2 strain, as shown in Fig. (1). The remaining gene segments of LAIV-N were from the A/Guangdong-Maonan/SWL1536/2019 (H1N1) strain (HA) and from MDV (PB2, PB1, PA, NP, M, and NS). The viable LAIV-N virus was rescued according to a previously developed protocol [27] as a result of Vero CCL81 electroporation with a cocktail of eight dual-promoter plasmid DNAs bearing all viral genome segments. LAIV-N was then propagated for 3 days at 33 °C in the allantoic fluid of 10-day-old embryonated chicken eggs. The clarified viral stock (processed *via* low-speed centrifugation) was aliquoted and maintained at -70°C until needed.

2.3. Hamster Study Design

The study was performed in 2025 and utilized female Golden Syrian hamsters (*Mesocricetus auratus*, 4-8 weeks old) obtained from Stezar cattery (Vladimir region, Russia). All experimental procedures were conducted following approval from the Institute of Experimental Medicine's local ethics committee (protocol 4/24, October 24, 2024) and in accordance with Directive 2010/63/EU [31].

The 20 animals weighing 80-100 g were maintained in a standard vivarium facility with free access to food and water. We used five animals per group as a minimal statistically relevant sample size, which were preliminarily screened in ELISA on 100 ng per well of rN to exclude the positive ones. No exclusions were made, and then animals were immunized with rN antigen 1:4 formulated with aluminum hydroxide (100 µg per hamster in a volume of 400 µL, intraperitoneally), with LAIV-N (10⁶ EID₅₀ per hamster in a volume of 100 µL, intranasally) or with SARS-FI 1:4 formulated with aluminum hydroxide (5 µg per hamster in a volume of 100 µL, intramuscularly). Importantly, the whole-virion SARS-FI vaccine, in addition to the N component, also contained quantitatively smaller amounts of spike protein. A control group obtained alum-adjuvanted PBS both intraperitoneally and intramuscularly. The intraperitoneal route of rN administration, its dose, and formulation with aluminum hydroxide were selected to induce a pronounced anti-N immune response, as was previously performed in a mouse model [11].

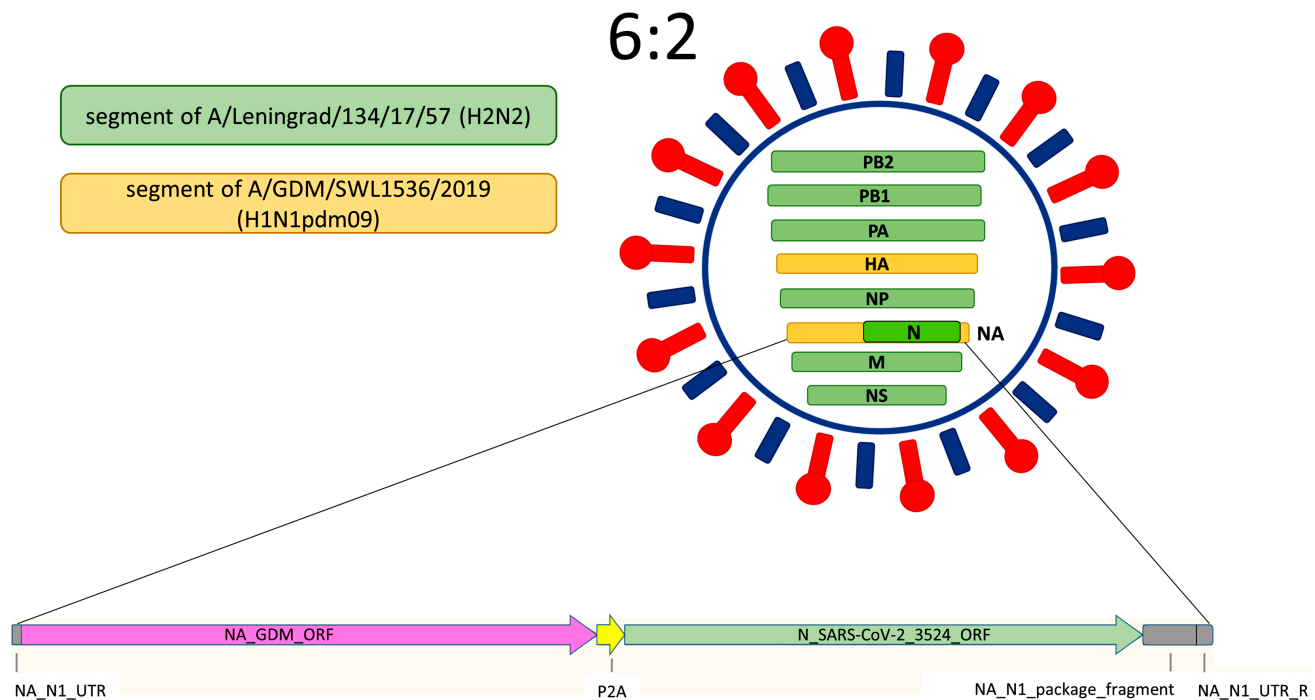


Fig. (1). The scheme of the LAIV-N virus contains the NA gene with N(B.1) insertion in the NA open reading frame, followed by the P2A self-cleavage site required for independent cell expression of the influenza NA component and the inserted gene [30].

As given in Fig. (2), on the 24th day after the boosting immunization, the hamsters were intranasally challenged with HCoV-19/Russia/StPetersburg-3524/2020 (B.1, Wuhan) virus at a dose of 10^5 TCID₅₀ (100 μ L) under light ether anesthesia. The challenge dose was chosen as inducing consistent infection without overwhelming lethality, as it was defined previously [32]. The progression of infection and associated changes in body weight were monitored over a six-day period post-inoculation. The following clinical parameters of the disease course were evaluated (0 - normal, 1 - reduced): coat performance, interaction with other animals, feed consumption, open field behavior, and reaction to being caught. All inoculations and measurements were conducted by qualified personnel following a strict protocol. Animals were assigned to the groups based on initial body weight to ensure similar mean values within each group. Samples were collected unblinded, except for those taken for histological study. The animals were marked with 0.5% picric acid, and cages were positioned at a distance to minimize potential confounding factors.

The airway replication rates were assessed as on the 6th day in aseptically dissected nasal turbinates and lungs, obtained from the hamsters humanely euthanized by ether overdose. We used TissueLyser LT (Qiagen, Hilden, Germany) equipped with the steel beads to homogenize the weighted tissues in PBS containing $1 \times$ AA. The viral titers were determined in Vero CCL81 cells 20 h after

inoculation by the previously described method [14] as focus-forming units (FFU) per mL. To count FFUs, we used the AID vSpot Spectrum system (Autoimmun Diagnostika GmbH, Germany).

One lung lobe was fixed in 10% buffered formalin solution (pH = 7.4) for 48 hours and further used for histological studies. Standard histological processing was performed on the samples using the Histo-Tek VP1 histoprocessor (Sakura, Japan), with subsequent embedding of the prepared specimens in paraffin. Thin sections (3 μ m) were prepared and stained with H&E solution according to standard protocol. MSB staining provided selective visualization: blood clots and erythrocytes appeared red, adventitial collagen was stained blue, and lymphocytes showed purple dying. Microscopic examination was performed using LEICA DM1000 equipment, with imaging and morphometric data acquisition conducted via ADF Image Capture 4.17 software. Semi-quantitative morphometric analysis was performed as published previously [32] and evaluated the involvement of airways, pulmonary parenchyma, and vascular system in pathogenesis. The degree of damage to the airways, pulmonary parenchyma, and vessel bed was calculated by the sum of scores of three evaluated pathology parameters: lesion area percentage, damage severity, and bronchiolar epithelium/pneumocyte type II hyperplasia. Histological evaluation was performed in a blinded manner by multiple pathologists.

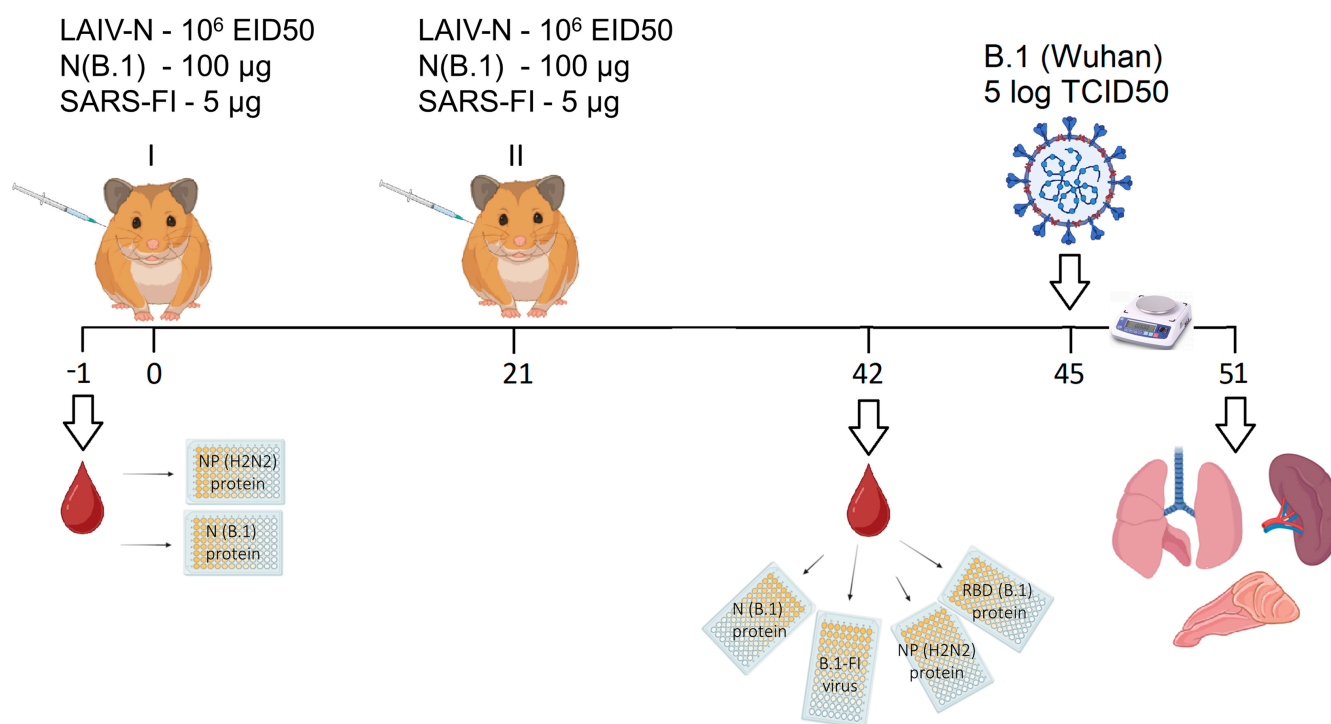


Fig. (2). A schematic representation of experimental design, immunizations, and subsequent evaluation of immunogenicity and protective efficacy of N-based vaccine candidates in a Syrian hamster model.

For evaluation of cell-mediated antiviral responses, spleen samples underwent ELISPOT analysis using the IFN- γ ELISPOT Plus kit (Mabtech, Hamburg, Germany) per manufacturer's protocol. The procedure involved suspending 500,000 strainer-filtered splenocytes in 150 μ L of CR-10 medium (RPMI supplemented with 10% FBS, 5 mM HEPES, 1 \times AA, and 50 μ M β -mercaptoethanol), which was then distributed into sterile U-bottom 96-well plates. Following the addition of PepTivator® SARS-CoV-2 Prot_N (Miltenyi Biotec, USA), the mixture was transferred to prewashed ELISPOT plates equilibrated with CR-10 medium. The 18-hour stimulation period was conducted at 37°C with 5% CO₂, after which anti-IFN- γ staining was performed using detection antibodies. The staining process was terminated by extensive water rinsing, and spot detection/counting was executed using the AID vSpot Spectrum system (Advanced Imaging Devices GmbH, Strassberg, Germany) in overnight-dried plates.

2.4. Assessment of Humoral Responses

Vaccine antigenicity was evaluated by enzyme-linked immunosorbent assay (ELISA) using the following coating antigens at a dose of 100 ng per well:

- sucrose gradient-purified formalin-inactivated SARS-CoV-2 (B.1) virus
- recombinant RBD protein of SARS-CoV-2 (B.1)
- recombinant NP protein of A/Leningrad/134/17/57 (H2N2)
- recombinant N protein of SARS-CoV-2 (B.1)

To perform ELISA, we first coated high-binding 96-well plates (JetBiofil, Guangzhou, China) with the inactivated virus or recombinant proteins overnight at +4 °C. On the following day, the plates were triple-washed with PBST (PBS supplemented with 0.05% Tween 20) and subsequently blocked by 1% bovine serum albumin (BSA) solution for 2 h. Two-fold serial dilutions of hamster sera were introduced into the wells, commencing at a 1:50 dilution ratio. Following a 1 h incubation period, HRP-conjugated goat anti-hamster IgG secondary antibodies (1:10000, BioRad, Hercules, CA, USA) were applied and incubated for 30 minutes. The plates were subsequently developed using 1-Step Ultra TMB-ELISA Substrate Solution (ThermoFisher Scientific, Waltham, MA, USA) for 15 minutes and measured at 450 nm on a xMark spectrophotometer (BioRad, Hercules, CA, USA). The serum IgG titer was determined as the maximal dilution at which the OD₄₅₀ value was twice the average OD₄₅₀ of control wells lacking the sera.

2.5. Statistical Analysis

The statistical data processing was performed using the GraphPad Prism 6.0 Software (GraphPad Software, San Diego, CA, USA). The Shapiro-Wilk test was used to evaluate the data's compliance with the normal distribution, and intergroup differences were assessed by one-way ANOVA with Tukey's multiple comparisons test. Statistical significance was defined as $p < 0.05$.

3. RESULTS

3.1. SARS-CoV-2-specific Humoral Immune Responses

The development of humoral immune responses as a result of immunizations (Fig. 3) was evaluated by ELISA screening on immobilized recombinant RBD (Fig. 3A), formalin-inactivated B.1 (Wuhan) coronavirus (Fig. 3B), and N antigen (Fig. 3C), as well as on influenza NP protein (Fig. 3D). The analysis of titration curves revealed that all vaccine prototypes were found to be immunogenic against the nucleocapsid protein (rN), except LAIV-N, which stimulated only antibody formation against the influenza NP antigen (Fig. 3), left panels). The same results were found by comparing the areas under the curve (AUCs) (Fig. 3), right panels). In general, signals in the groups that received the SARS-FI and rN vaccines, when screened on the immobilized N antigen, were 7-10 times higher when expressed in AUC values and 2-2.5 times higher when expressed in OD₄₅₀ values (Fig. 3C).

The data concerning the LAIV-N immunogenicity were expected due to the specific design of this vaccine prototype, where the N insertion contained in the NA segment *via* the P2A site undergoes degradation in the proteasome and further stimulates T-cell responses in the form of epitopes. At the same time, the anti-N immunogenicity of the other studied vaccines appeared to be slightly different when analyzed on the same antigen.

The fact of the humoral immunity stimulation in response to immunizations was further considered as a promising basis to protect animals from infection caused by the homologous SARS-CoV-2 variant.

3.2. Protection against SARS-CoV-2 (B.1) Challenge

We further tested if the rN, LAIV-N, or SARS-FI vaccines could protect Syrian hamsters from a high dose of homologous SARS-CoV-2 virus (B.1 variant), *i.e.* evaluated the protective efficacy (expected as a partial viral load reduction) of our vaccine prototypes. The challenge was performed intranasally four weeks following the second vaccination dose. The evaluation results are presented in Fig. (4A-F). In case of SARS-FI, significant reduction in viral load of B.1 (Wuhan) was detected in lung specimens, as shown in Fig. (4A). Significantly lower titers of infectious virus were detected in nasal turbinate specimens obtained from animals immunized with SARS-FI and LAIV-N preparations than in the upper airways of animals from the placebo group (Fig. 4B, C). Interestingly, despite an unpronounced reduction in the SARS-CoV-2 pulmonary replication and vulnerability to weight loss in the LAIV-N vaccinated animals (Fig. 4D, F), Syrian hamsters immunized with this vaccine prototype exhibited significantly milder clinical signs of SARS-CoV-2 infection compared to the control group animals, as demonstrated in Fig. (4E).

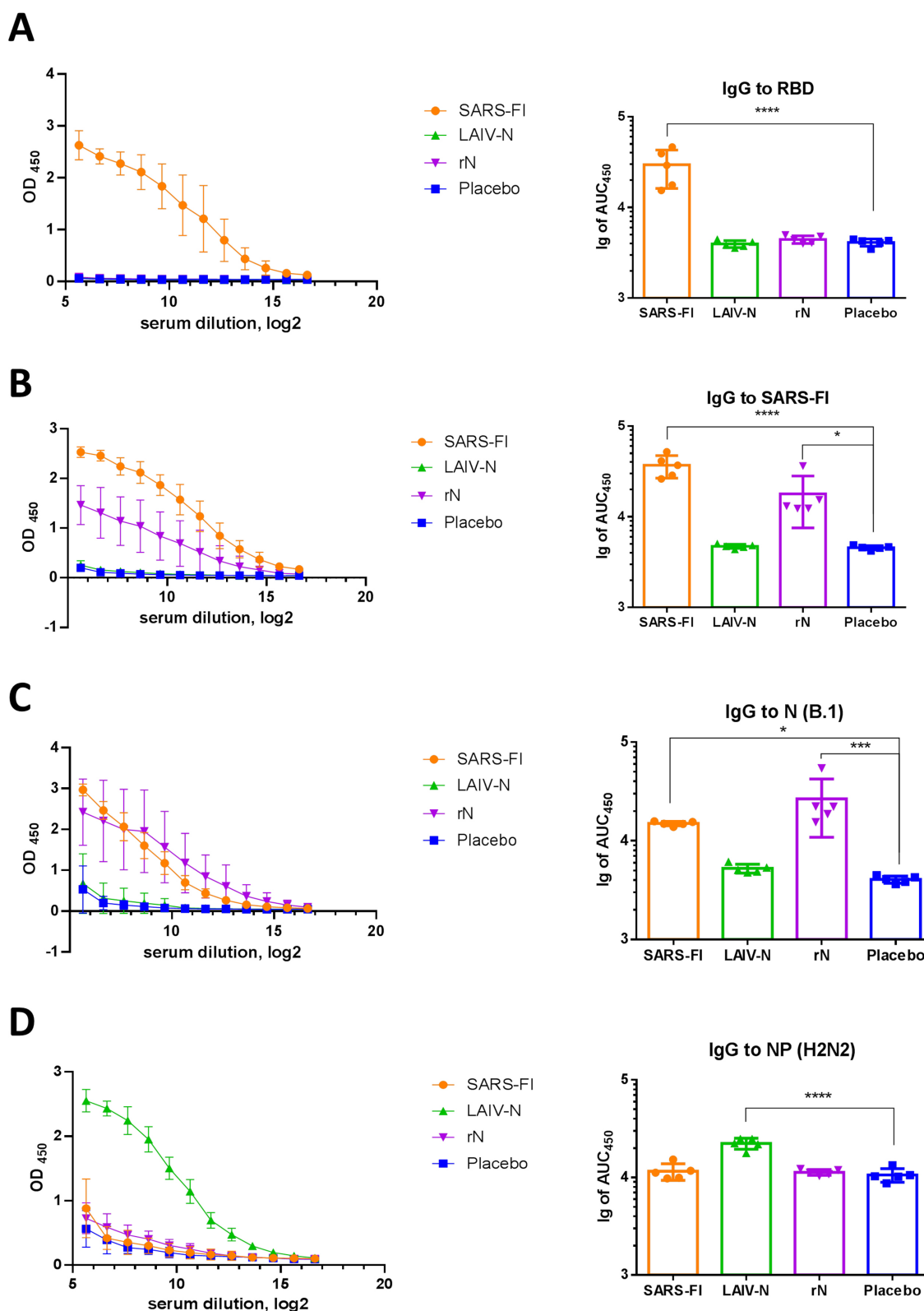


Fig. (3). Serum IgG antibody responses in hamsters immunized with the studied vaccines. OD₄₅₀ values (**left panels**) and AUC values (**right panels**) were revealed in ELISA against RBD antigen (**A**), formalin-inactivated SARS-CoV-2 (**B**), recombinant N (B.1) protein (**C**), and recombinant influenza NP (H2N2) protein (**D**). Antibody levels were assessed at day 42, following administration of two vaccine doses. **** - $p < 0.0001$, *** - $p < 0.001$, * - $p < 0.05$ (one-way ANOVA with pos-hoc Tukey's test).

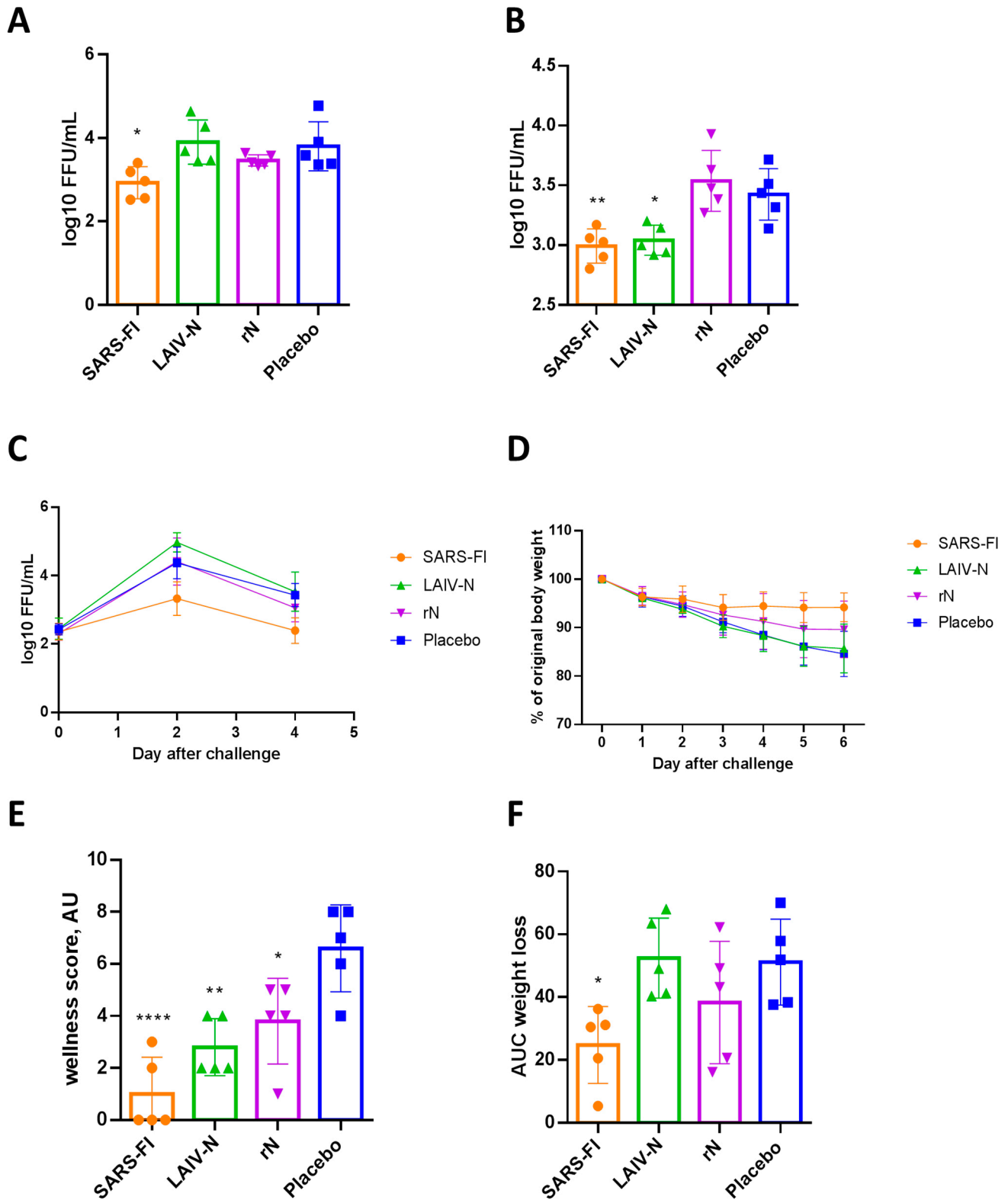


Fig. (4). Protective efficacy of rN, LAIV-N and SARS-FI against 10^5 TCID₅₀ of SARS-CoV-2 (B.1). Viral titers in lung tissues (A) and nasal turbinates (B) and on day 6 post-challenge are shown, as well as replication curves in nasal washes (C), individual body weight dynamics (D), cumulative sum of clinical symptom scores (E) and AUCs of weight loss (F). **** - $p < 0.0001$, ** - $p < 0.01$, * - $p < 0.05$ (one-way ANOVA with post-hoc Tukey's test).

Histological examination of the lung tissue of naive hamsters (Fig. 5A) showed a normal structure of the airways and respiratory section of the lungs. The airiness of the lungs exceeded 85%. In bronchioles and large bronchi, a moderate number of mucus-producing cells and normal proliferation of epithelium were noted (mean score value = 1). The capillaries contained single erythrocytes, the lumen of large vessels did not contain thrombi, and the vessel walls were uniform in thickness and structure. The endothelial lining of pulmonary arteries had a normal structure (mean score value = 1.8).

In the placebo group, a decrease in lung airiness of up to 40% was noted due to the inflammation and thickening of the alveolar walls caused by SARS-CoV-2 infection (mean score value = 5.6). The vascular damage was total (mean score value = 7.2), as each lung lobe submitted for examination showed intraluminal dense fibrin thrombi (both postmortem and intravital), endothelial proliferation, edema, and thickening of the media, as well as an adventitial edema with lymphocyte infiltration. The perivascularitis was detected around each vessel at 200x magnification.

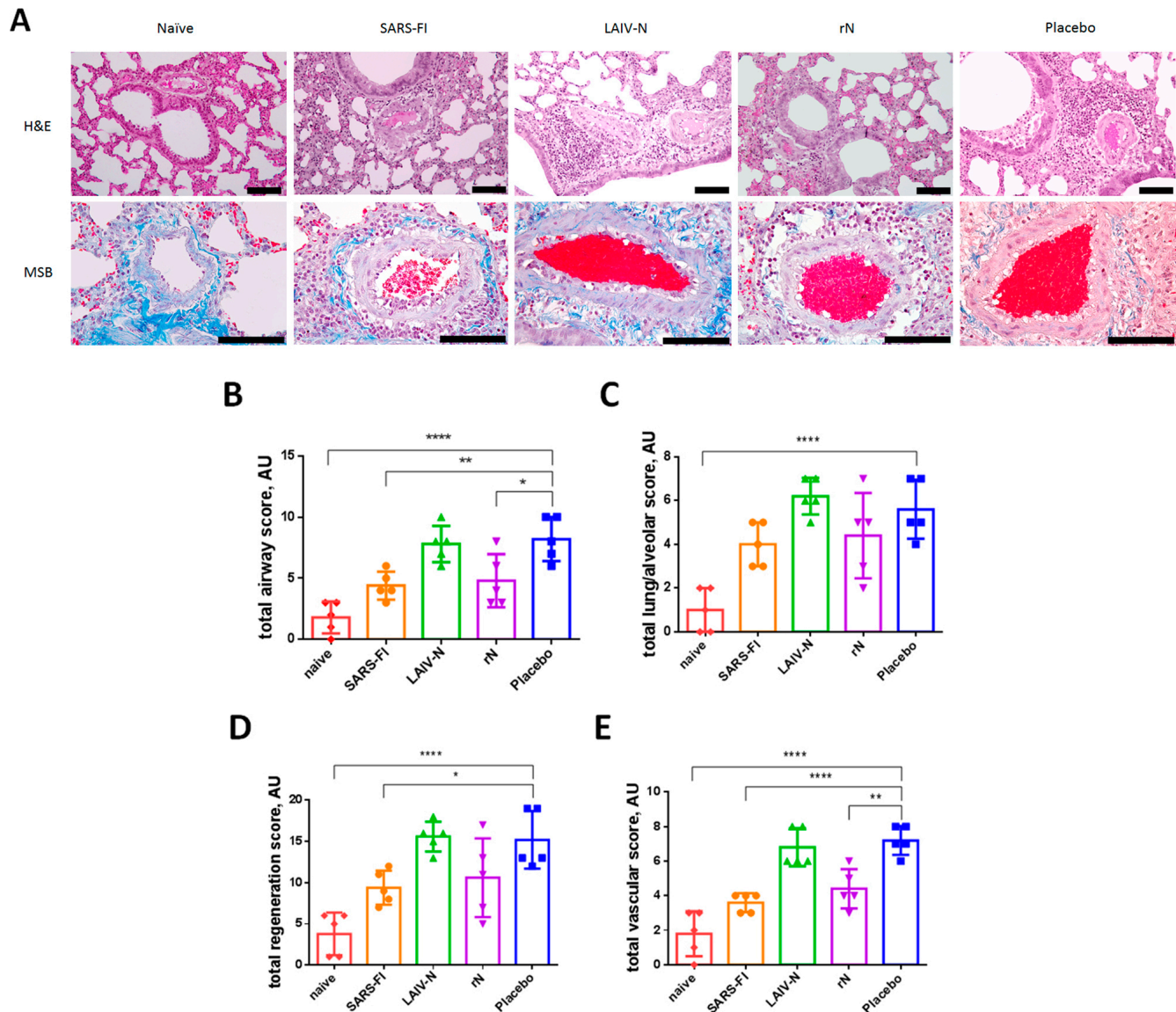


Fig. (5). Histopathological assessment of the lung tissue samples from immunized hamsters collected on day 6 after challenge with B.1 (Wuhan). **A** — representative micrographs of H&E- (shown at 200× magnification) or MSB-stained lung sections (shown at 400× magnification) of animals on day 6 after challenge, scale bar: 100 μm; **B** — semi-quantitative assessment of bronchial and bronchiolar lesions; **C** — semi-quantitative assessment of pulmonary-alveolar pathological changes; **D** — semi-quantitative assessment of bronchiolar epithelial/type II pneumocytic hyperplasia; **E** — vessel bed semi-quantitative lung assessment. **** $p < 0,0001$, ** $p < 0,01$, * $p < 0,05$ (one-way ANOVA with Tukey's post hoc test).

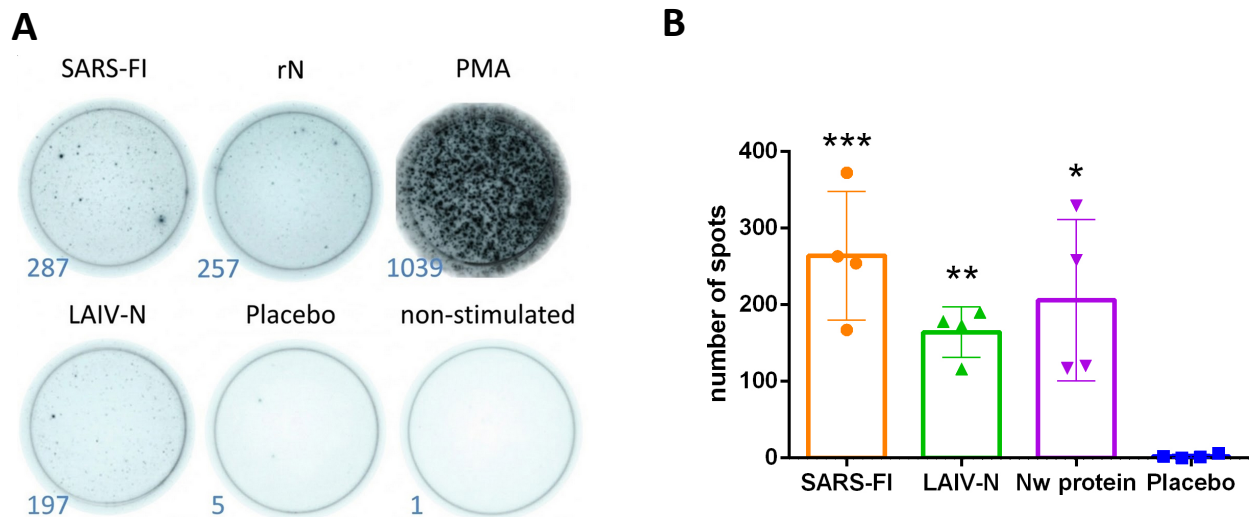


Fig. (6). Representative well photos (A) and intensities of generation of IFN- γ -secreting N-specific splenocytes isolated on day 6 after infection with SARS-CoV-2 (B.1, Wuhan) in three groups of immunized Syrian hamsters (B). The stimulations were performed with PepTivator®, followed by detection of IFN- γ -secreting cells by the Hamster IFN- γ ELISpot Plus kit. *** - $p < 0.001$, ** - $p < 0.01$, * - $p < 0.05$ (one-way ANOVA with pos-hoc Tukey's test).

The changes in the lung parenchyma and vessels in hamsters from the LAIV-N group were similar to those in the mock animals (mean score value = 7.8 vs 8.2). In two Syrian hamsters out of five, the changes were severe, while in three animals, they were less pronounced. The airiness of the lungs varied from 60-75% to 20-40% due to the inflammation and thickening of the alveolar walls caused by the virus infection (mean score value = 6.2). From the vascular side, changes were similar to those in the Placebo group (mean score value = 6.8).

In the rN group, damages of the lung parenchyma and vessels was less pronounced (mean score value = 4.8). In one hamster out of five, the tissue changes were severe (50%), and in four animals, they were moderate (10-20% of damage), and the airiness of the lungs varied from 50% to 90% (mean score value = 4.4). The changes in the vessel performance were unpronounced (mean score value = 4.4); the perivascularitis was diagnosed in the area of inflammatory foci, and the intraluminal thrombi were mixed, partly due to the euthanasia method (recently formed).

In the lungs of Syrian hamsters from the SARS-FI group, pathological changes were minimal compared to all other animals (mean score value = 4.3). The parenchyma airiness was reduced to only 75-90% (mean score value = 4). The inflammatory processes were characterized by the focal thickening of the alveolar walls; a moderate activation of bronchiolar epithelium proliferation was noted. The vascular lesions were manifested in the form of thrombi (one per three vessels in the field of view at 200x magnification), with moderate up to three layers of inflammatory cells around the vessels (a perivascularitis typical for SARS-CoV-2 infection, mean score value = 3.6).

Semi-quantitative assessment of lung tissue lesions (Fig. 5B-E) in hamsters from the placebo and LAIV-N groups showed a marked degree of bronchial and bronchiolar involvement in the pathogenesis (mean score values = 8.2

and 7.8, respectively, (Fig. 5B) along with the detectable severe pulmonary-alveolar pathological changes (mean score values = 5.6 and 6.2, respectively, (Fig. 5C), progression of bronchiolar epithelial hyperplasia and/or type II pneumocyte hyperplasia with formation of syncytium or atypical multinucleated cells (mean score values = 15.2 and 15.6, respectively, (Fig. 5D) and vascular lesions (mean score values = 7.2 and 6.8, respectively, (Fig. 5E) compared to naïve animals (mean score values for listed assessments = 1.8, 1, 3.8 and 1.8, respectively). SARS-FI vaccination provided the best pulmonary tissue protection, as all the assessments showed significant score differences with the placebo group (mean score values for the listed assessments = 4.4, 4, 9.4, 3.6, respectively). Surprisingly, a weak protective effect of rN immunization against homologous infection was found (mean score values for listed assessments = 4.8, 4.4, 10.6, 4.4, respectively); however, despite better lung tissue performance in this group, rN vaccination did not significantly prevent SARS-CoV-2 (B.1) replication (Fig. 4A).

3.3. Assessment of Cell-mediated Immunity to Influenza and SARS-CoV-2 Antigens

The evaluation of cell-mediated immune responses was performed on hamster splenocytes collected six days post-infection with 10^5 TCID₅₀ of the B.1 (Wuhan) virus. Evaluation of T-cell responses after the *in vitro* stimulation of immune cells by purified SARS-CoV-2 virus (MOI 0.1) or by overlapping N peptide pool (PepTivator® SARS-CoV-2 Prot_N) performed in ELISPOT assay (detection examples are presented in Fig. (6A)) showed that in the first case all vaccine variants induced a significant generation of N-specific splenocytes, which secreted IFN- γ in response to stimulation with peptides covering the entire N sequence (Fig. 6B). Although SARS-FI was found to be predominantly immunogenic, the observed ability of LAIV-

N to stimulate the generation of N-specific splenocytes matches our previously published results demonstrating augmented T-cell responses to recombinant LAIVs bearing foreign immunodominant T-cell epitopes [33]. Notably, the inserted N gene of SARS-CoV-2 comprised a prolonged cassette that might contain hamster-specific T-cell epitopes. Importantly, the data obtained reflect the N-specific post-challenge T-cell responses, and not the pre-challenge vaccine-induced changes in T-cell levels.

Thus, the immunogenicity study in Syrian hamsters showed that the modified LAIV bearing the full-length gene of SARS-CoV-2 stimulates humoral immunity to the recombinant NP of H2N2 influenza virus, as well as T-cell responses to SARS-CoV-2. At the same time, SARS-FI and recombinant N-based prototype (rN) were found to be able to provoke both T- and B-cellular N-specific responses.

4. DISCUSSION

The conserved structure and robust immunogenic properties of the SARS-CoV-2 nucleocapsid protein make it an attractive target for developing broadly protective COVID-19 vaccines [34]. In the present study, the protective potential of the N protein was assessed by its delivery to the organism using different routes. Apparently, intraperitoneal administration of recombinant N protein induced robust antibody responses, although these levels were insufficient to reduce viral loads in the respiratory tissues of immunized hamsters. On the other hand, N protein delivered by the attenuated influenza vector *via* the intranasal route provoked responses different from those induced by SARS-FI, which reflects that the mucosal delivery platform, compared to systemic presentation of inactivated vaccine, alternatively stimulates immunity. Specifically, LAIV-N did not produce anti-N serum antibodies, but, similar to SARS-FI, it stimulated N-specific cell-mediated immune responses and protected animals, partially reducing the viral replication in the upper respiratory tract. This may be explained by the need to engage several factors which may be provoked by the LAIV as carrying vector for intranasal administration of combined vaccines, such as stimulation of mucosal immunity [35, 36] including local T-cell component [37], generation of long-lived cross-reactive tissue resident memory T-cells [38, 39], innate immune processes [40], formation of more functionally active antibodies compared to the induced by inactivated influenza vaccine [41] and activation of the trained innate immunity [42, 43]. Presumably, immunization with LAIV-N ensures the delivery of the immunogenic T-cell epitopes straight to target airway cells, potentially fostering effective T-cell-mediated antiviral immunity. Notably, spike-based vaccines are also known for their ability to stimulate T-cell immune responses comparable to those elicited by natural infection. However, this data cannot be directly translated to the studied vaccines, as the mentioned reports assessed T-cell responses stimulated by spike peptides, while the present study was focused on the N protein immunogenicity. It is also important to mention the well-known ability of the LAIV vector alone to induce

an interferon-mediated antiviral state [40] and to significantly increase the levels of cytokine-producing T cells [27], which may additionally provide antiviral protection upon immunization with the LAIV-N vaccine, although expression of the N component has been experimentally demonstrated.

Similar to the worldwide use of LAIV, generally licensed for individuals between 2 and 49 years old [44,45], LAIV-N prototype also possesses obvious translational potential and is expected to be similarly safe, so its production could be scaled for human use in case of successful passing of clinical trials. In addition, a spike-expressing construct may be introduced into one of the genetic segments of this vaccine in the future to obtain a bivalent mucosal vaccine, which will provide the production of neutralizing antibodies and improve the protective efficacy of this prototype.

The fact that rN elicited strong immune responses but failed to inhibit viral replication creates some discrepancy between immunogenicity and protective potential, which may be explained by the undesirable effects of intensively provoked anti-N immune responses. Clear evidence of autoimmune properties [46], the ability to induce pro-inflammatory antibody-dependent infection enhancement [47] as well as the association of reactivity with lower-airway radiological abnormalities [48] have previously been described for anti-N IgG antibodies. These data are in line with our finding that LAIV-N showed minimal humoral response but significantly reduced replication rates and clinical symptoms. T-cell mediated protection may be the most likely explanation for this phenomenon. At the same time, as it was revealed from the challenge study, rN improved lung pathology but did not reduce viral replication, demonstrating a distinction between clinical and virological protection. The improved histological picture revealed after the challenge in animals from the rN group may be associated with some mechanisms like antibody-mediated clearance of infected cells and activation of T-cellular immunity, as well as with adjuvant bias or induction of innate responses (*e.g.*, complement activation or antibody-dependent cellular cytotoxicity/phagocytosis) mediated by the anti-N antibodies [10].

A pronounced cross-reactivity of anti-N immunoglobulins has previously been demonstrated both in studies of sera from COVID-19 convalescents [49] and by comparing the antigenic properties of N proteins of different SARS-CoV-2 lineages in a mouse model [11]. A cross-reactivity of N-specific T cells stimulated by B.1 and B.1.617.2 variants has been previously demonstrated in a hamster model while studying another bivalently linked vaccine prototype [27].

The development of N-based universal COVID-19 vaccines to strain-independently prevent SARS-CoV-2 infection spread seems to be a promising way to increase vaccine cross-protectiveness and cost-effectiveness, and this premise is not new. A number of such experimental prototypes have been recently proposed, first of all several candidates based on recombinant N protein expressed in *E. coli* cells and emulsified with potent adjuvants. In their

study, Ghaemi *et al.* developed a multi-component vaccine platform utilizing saponin adjuvant combined with recombinant RBD domain from spike protein and N antigen of SARS-CoV-2 (B.1). Triple subcutaneous immunization of mice resulted in robust neutralizing IgG antibody production, substantial expansion of CD4+ and CD8+ T cell subsets, and induction of polarized Th1/Th2 immune responses [21]. The study by Thura *et al.* [50] focused on evaluating the protective properties of full-length and fragmented N protein as potential vaccine components. The research demonstrated their strong immunogenic capacity and ability to induce prolonged N-specific humoral responses in a mouse model. The development of OVX033, a highly immunogenic vaccine formulation, involved the fusion of the complete N protein from SARS-CoV-2 variant B.1 with the heptamerization domain of OVX313. Employing technology analogous to a previously reported universal influenza vaccine utilizing multimeric NP antigen [51], this vaccine was engineered for universal protection against sarbecovirus infections. In a Syrian hamster model, vaccination with this prototype elicited pronounced N-specific antibody production. Although these antibodies did not exhibit neutralizing activity, they contributed to Fc-mediated protective responses and conferred cross-protection against SARS-CoV-2 variants B.1, B.1.617.2, and B.1.1.529 [23]. Ozcengiz *et al.* proposed a novel combined vaccine formulation comprising two immunogenic spike protein sites (P1 and P2) along with a full-length N-antigen, adjuvanted with aluminum hydroxide, either alone or in combination with monophosphoryl lipid A. This vaccine demonstrated efficacy in inducing anti-P1, anti-P2, and anti-N IgG antibodies, including neutralizing ones, as well as IFN- γ -secreting T cells in a murine model. Notably, the formulation containing monophosphoryl lipid A was specifically suggested for elderly populations due to its ability to promote a Th1-type immune response [52]. Feng *et al.* also suggested utilizing the full-length recombinant N protein of SARS-CoV-2 as a basis for a universal vaccine. This proposal was based on two key observations: the correlation between anti-N antibody titers and COVID-19 disease severity, and the demonstrated high immunogenicity of the N protein in mice. Vaccination with this prototype resulted in the active systemic production of N-specific IgG and IgM antibodies, along with IFN- γ [22]. In their research, Nazarian *et al.* conducted immunization experiments using three distinct adjuvants (alum, AS03, and Montanide) in mice, rabbits, and primates. The immunization regimen involved a combination of recombinant RBD, truncated Spike protein (lacking the N-terminal domain S1), and full-length N-protein. The study demonstrated the absence of toxicity across all tested species, robust generation of specific IgG antibodies, and pronounced induction of effector T lymphocytes. Notably, the strongest immune responses were observed with SARS-CoV-2 antigens adjuvanted with AS03 and Montanide [53]. The Convacell vaccine, consisting of the recombinant N protein of bacterial origin and a squalene adjuvant, showed safety and immunogenicity in mouse models of the BALB/c and SCID lines, rabbits, hamsters,

and primates, inducing intense N-specific antibody formation, Th1/Th2-type cytokine responses in mice and rabbits, and active generation of anti-N CD4+/CD8+ T cells in non-human primates. This formulation exhibited protective properties in vaccinated animals by minimizing pulmonary tissue damage, inhibiting viral replication kinetics, and reducing body mass loss upon the SARS-CoV-2 challenge, suggesting effective antiviral immunity [20]. To date, only this N antigen-based vaccine has been approved for clinical use, with comparable increases in IFN- γ and IL-2-secreting CD4+ and CD8+ T cells in vaccinated volunteers and COVID-19 convalescents in response to stimulation with N protein variants B.1, B.1.617.2, and B.1.1.529 [20].

Yilmaz *et al.* developed an innovative vaccine prototype utilizing the virus-like particles (VLPs) that carried S, N, M, and E antigens and exhibited morphological similarity to SARS-CoV-2 virions. The most effective immunogenic response, characterized by robust induction of specific humoral and Th1-type T-cell responses, was achieved through alum adsorption of the particles combined with the CpGOND-K3 adjuvant. Evaluation of protective efficacy in the K18 hACE2 transgenic mouse model demonstrated significant reductions in both viral load and lung lesions among vaccinated animals [54]. In the animal models, novel glyconanoparticles synthesized on the basis of full-length recombinant N protein and high-affinity dextran derivatives successfully induced antibody production as well as cytotoxic lymphocytes with prolonged activity, which further possessed cross-reactivity against various SARS-CoV-2 strains *in vitro* [55].

A number of studies on N-bearing vector vaccines have also been reported. So, Dangi *et al.* conducted research to enhance the immunogenicity of a vaccine based on attenuated human adenovirus type 5 (Ad5) carrying the S gene. It was supplemented with an additional Ad5 vector expressing the N protein, and the results demonstrated a significant increase in CD4+ and CD8+ T cell counts, elevated specific antibody titers in vaccinated K18-hACE2 mice, and a notable reduction in the severity of virus-induced brain lesions [24]. A similar vaccine formulation utilizing adenovirus type 5 (Ad5) vector carrying the N gene instead of the S gene demonstrated protective efficacy in preclinical studies. The research was conducted using Syrian hamster and K18-hACE2 transgenic mice models, and demonstrated successful induction of protective immunity provided by rapid mobilization of memory CD8+ T cells during challenge infection [56]. An alternative approach to the N antigen delivery involves the use of a vesicular stomatitis virus (VSV) vector carrying both the S- and N-expressing constructs. Preclinical studies demonstrated that intranasal pre-immunization of the Syrian hamsters provided protection against different SARS-CoV-2 variants, and the intranasal route proved to be effective in preventing infection, while intramuscular administration did not yield protective results [25]. Routhu *et al.* developed a novel vaccine formulation utilizing a modified vaccinia Ankara (MVA) vector that included the

N gene and Spike protein gene bearing a defective furin cleavage site. When administered intramuscularly (the most effective route of administration), this vaccine candidate promoted systemic excretion of SARS-CoV-2 variants in hamsters [57]. Trivalent candidate vaccines against COVID-19 carrying the S-1, N, and RdRp genes, based on human or chimpanzee adenoviral vectors have also been proposed. A single administration of the vaccine in mice demonstrated the following immunological effects: induction of both local and systemic specific humoral responses, generation of resident mucosal memory T cells (TRM), and protection against the evolutionarily distant SARS-CoV-2 variants [57]. A candidate vaccine consisting of a mixture of replication-defective Parapox viruses carrying the N or S genes was named Prime-2-CoV_Beta. This combined vaccine prototype induced an active formation of neutralizing anti-S antibodies and prevented increased viral load and lung and upper respiratory tract tissue damage in prevaccinated animals in a challenge study [26]. Recent studies have focused on the construction of a novel vaccine platform, wherein the ORFs of NS [58] and NA [27] of LAIV serve as a carrier for N-protein gene fragments. The resulting vaccine formulations have demonstrated remarkable immunogenicity profiles, characterized by potent T-cell responses and significant protective efficacy against both SARS-CoV-2 and influenza virus infections.

Despite numerous previous studies on the immunogenicity and protective potential of N-bearing vaccines, our work advances the field by conducting a comparative analysis of the effectiveness of several vaccine platforms and provides new insights regarding the correlation of immunogenicity and protective potential, explaining the mechanisms of responses against the N antigen.

CONCLUSION

The study revealed that vaccines based on the N(B.1) antigen, consisting of a recombinant N antigen (rN) and a whole virion inactivated SARS-CoV-2 (SARS-FI), were the most immunogenic, eliciting strong B- and T-cell responses. At the same time, immunization with the SARS-FI vaccine and the vector-based LAIV-N vaccine protected respiratory tissues, body weight, and well-being of animals from homologous infection. Although rN injection resulted in lung tissue performance similar to that of naïve animals, it was unable to prevent viral replication in the airways. The data obtained will help to better understand the mechanisms of the immune responses against the N component of SARS-CoV-2, and it will accelerate the development of universal COVID-19 vaccines. Here, homologous B.1 challenge was used as a baseline for platform evaluation, and further work will focus on analyzing the effectiveness of vaccines based on the N(B.1) strain against heterologous challenges, as well as studying the efficacy of alternative modified LAIVs that carry the N-insertion or its fragments in other gene segments.

Undoubtedly, our study has a number of limitations. First, we operated with small sample sizes, although we managed to find statistically significant intergroup

differences. Next, the longevity of immune responses induced by three vaccine prototypes was not evaluated, but will be studied further, and in the case of LAIV-N is expected to be the same for the well-studied classical LAIV viruses. Furthermore, N-specific T cells were not immunophenotyped (ICS analyzed) due to the commercial unavailability of fluorescently labeled anti-hamster antibodies; however, the hamster model currently represents the most suitable tool for *in vivo* SARS-CoV-2 studies, and we detected robust anti-N cell-mediated responses, although the work was predominantly focused on the immunogenicity and protective potential of the vaccines. Another limitation of the study is the lack of immunohistochemistry; this would have allowed for visualization of foci of SARS-CoV-2 replication in the various lung parts and evaluation of the impacts of the studied vaccines on the reduction and redistribution of the viral propagation in this organ. Next, notably, the hamster model, being an excellent tool for upper airway infection studies, may not fully recapitulate severe human COVID-19 pathology. Finally, we didn't evaluate mucosal IgA levels or innate immune mechanisms as well as the protective efficacy of our prototype N(B.1)-based vaccines against evolutionarily distant SARS-CoV-2 variants (as only homologous challenge with B.1 virus was performed), but a heterologous challenge will be comprehensively investigated in upcoming studies.

AUTHORS' CONTRIBUTIONS

The authors confirm contribution to the paper as follows: A.R., I.K. and I.I.-S.: Conceptualization; A.R., E.B., E.S. and I.I.-S.: Methodology; A.R. and I.I.-S.: Software; A.R., E.B. and E.S.: Validation; A.R., I.K. and P.P.: Formal analysis; A.R., E.B., P.P., E.S. and A.K.: Investigation; A.R., I.K. and K.S.: Resources; A.R., E.B., I.K. and P.P.: Data curation; A.R., I.K. and K.S.: Writing—original draft preparation; A.R., L.R. and I.I.-S.: Writing—review and editing; A.R. and A.K.: Visualization; I.K., I.I.-S., K.V.S. and L.R.: Supervision; I.I.-S., K.V.S. and L.R.: Project administration; A.R.: Funding acquisition. All authors read and approved the final manuscript.

LIST OF ABBREVIATIONS

rN	= N protein
LAIV-N	= N-expressing live attenuated influenza vaccine
ATCC	= American Type Culture Collection
AA	= antibiotic-antimycotic
MDV	= master donor virus
FFU	= focus-forming units

ETHICS APPROVAL AND CONSENT TO PARTICIPATE

The study was approved by the Ethics Committee of the Institute of Experimental Medicine (protocol No. 4/24, dated 24 October 2024).

HUMAN AND ANIMAL RIGHTS

This study adheres to internationally accepted standards for animal research, following the 3Rs principle. The ARRIVE guidelines were employed for reporting experiments involving live animals, promoting ethical research practices.

All the animal experimentations were performed in accordance with Directive 2010/63/EU guidelines.

CONSENT FOR PUBLICATION

Not applicable.

AVAILABILITY OF DATA AND MATERIALS

The data supporting the findings of the article are available in the Yandex Disk at https://disk.360.yandex.ru/d/_nNo-gDeBX6H-g.

FUNDING

This research was supported by the Russian Science Foundation [grant number 24-75-00010].

CONFLICT OF INTEREST

The author, Irina Kiseleva, is the Editor in Chief of The Open Microbiology Journal.

ACKNOWLEDGEMENTS

The authors thank Yana Orshanskaya from the Smorodintsev Research Institute of Influenza for her technical assistance with histological processing.

REFERENCES

- [1] Worldometer of COVID-19 coronavirus pandemic. 2025.2025. Available at: <https://www.worldometers.info/coronavirus/>
- [2] Scharf LG, Adeniyi K, Augustini E, *et al.* Monitoring and reporting the US COVID-19 vaccination effort. *Vaccine* 2024; 42(Suppl 3): 125495-502. <http://dx.doi.org/10.1016/j.vaccine.2023.12.005> PMID: 38097453
- [3] Laniece Delaunay C, Mazagatos C, Martínez-Baz I, *et al.* VEBIS Primary Care Vaccine Effectiveness Group. COVID-19 vaccine effectiveness in autumn and winter 2022 to 2023 among older Europeans. *JAMA Netw Open* 2024; 7(7): e2419258-270. <http://dx.doi.org/10.1001/jamanetworkopen.2024.19258> PMID: 38949812
- [4] Hadj Hassine I. Covid-19 vaccines and variants of concern: A review. *Rev Med Virol* 2022; 32(4): e2313. <http://dx.doi.org/10.1002/rmv.2313> PMID: 34755408
- [5] Bessa LM, Guseva S, Camacho-Zarco AR, *et al.* The intrinsically disordered SARS-CoV-2 nucleoprotein in dynamic complex with its viral partner nsp3a. *Sci Adv* 2022; 8(3): eabm4034-4045. <http://dx.doi.org/10.1126/sciadv.abm4034> PMID: 35044811
- [6] McBride R, Van Zyl M, Fielding B. The coronavirus nucleocapsid is a multifunctional protein. *Viruses* 2014; 6(8): 2991-3018. <http://dx.doi.org/10.3390/v6082991> PMID: 25105276
- [7] Bai Z, Cao Y, Liu W, Li J. The SARS-CoV-2 nucleocapsid protein and its role in viral structure, biological functions, and a potential target for drug or vaccine mitigation. *Viruses* 2021; 13(6): 1115-27. <http://dx.doi.org/10.3390/v13061115> PMID: 34200602
- [8] Grifoni A, Weiskopf D, Ramirez SL, *et al.* Targets of T cell responses to sars-cov-2 coronavirus in humans with covid-19 disease and unexposed individuals. *Cell* 2020; 181(7): 1489-1501.e15. <http://dx.doi.org/10.1016/j.cell.2020.05.015> PMID: 32473127
- [9] Peng Y, Mentzer AJ, Liu G, *et al.* Oxford Immunology Network Covid-19 Response T cell Consortium; ISARIC4C Investigators. Broad and strong memory CD4⁺ and CD8⁺ T cells induced by SARS-CoV-2 in UK convalescent individuals following COVID-19. *Nat Immunol* 2020; 21(11): 1336-45. <http://dx.doi.org/10.1038/s41590-020-0782-6> PMID: 32887977
- [10] Rak A, Bazhenova E, Prokopenko P, *et al.* Protective potential and functional role of antibodies against SARS-CoV-2 nucleocapsid protein. *Antibodies* 2025; 14(2): 45-62. <http://dx.doi.org/10.3390/antib14020045> PMID: 40558099
- [11] Rak A, Gorbunov N, Kostevich V, *et al.* Assessment of immunogenic and antigenic properties of recombinant nucleocapsid proteins of five sars-cov-2 variants in a mouse model. *Viruses* 2023; 15(1): 230-43. <http://dx.doi.org/10.3390/v15010230> PMID: 36680269
- [12] Dutta NK, Mazumdar K, Gordy JT. The nucleocapsid protein of SARS-CoV-2: A target for vaccine development. *J Virol* 2020; 94(13): e00647-20. <http://dx.doi.org/10.1128/JVI.00647-20> PMID: 32546606
- [13] Oronsky B, Larson C, Caroen S, *et al.* Nucleocapsid as a next-generation COVID-19 vaccine candidate. *Int J Infect Dis* 2022; 122: 529-30. <http://dx.doi.org/10.1016/j.ijid.2022.06.046>
- [14] Rak A, Matyushenko V, Prokopenko P, *et al.* A novel immunofluorescent test system for SARS-CoV-2 detection in infected cells. *PLoS One* 2024; 19(5): e0304534-45. <http://dx.doi.org/10.1371/journal.pone.0304534> PMID: 38820303
- [15] Beavis AC, Li Z, Briggs K, *et al.* Efficacy of parainfluenza virus 5 (PIV5)-vectored intranasal COVID-19 vaccine as a single dose primer and booster against SARS-CoV-2 variants. *J Virol* 2025; 99(4): e01989-24. <http://dx.doi.org/10.1128/jvi.01989-24> PMID: 40116505
- [16] Lakhri F, Poupée-Beaugé A, Boursin F, *et al.* Intranasal spike and nucleoprotein fusion protein-based vaccine provides cross-protection and reduced transmission against SARS-CoV-2 variants. *NPJ Vaccines* 2025; 10(1): 75-92. <http://dx.doi.org/10.1038/s41541-025-01123-y> PMID: 40251181
- [17] Rabdano SO, Ruzanova EA, Vertyachikh AE, *et al.* N-protein vaccine is effective against COVID-19: Phase 3, randomized, double-blind, placebo-controlled clinical trial. *J Infect* 2024; 89(5): 106288-95. <http://dx.doi.org/10.1016/j.jinf.2024.106288> PMID: 39341405
- [18] Sultana R, Stahelin RV. Strengths and limitations of SARS-CoV-2 virus-like particle systems. *Virology* 2025; 601: 110285-96. <http://dx.doi.org/10.1016/j.virol.2024.110285> PMID: 39536645
- [19] Alsuwairi FA, Alsaleh AN, Alsanea MS, *et al.* Association of SARS-CoV-2 nucleocapsid protein mutations with patient demographic and clinical characteristics during the delta and omicron waves. *Microorganisms* 2023; 11(5): 1288-306. <http://dx.doi.org/10.3390/microorganisms11051288> PMID: 37317262
- [20] Rabdano SO, Ruzanova EA, Pletyukhina IV, *et al.* Immunogenicity and *in vivo* protective effects of recombinant nucleocapsid-based SARS-CoV-2 vaccine convacell®. *Vaccines* 2023; 11(4): 874-93. <http://dx.doi.org/10.3390/vaccines11040874> PMID: 37112786
- [21] Ghaemi A, Roshani Asl P, Zargaran H, *et al.* Recombinant COVID-19 vaccine based on recombinant RBD/Nucleoprotein and saponin adjuvant induces long-lasting neutralizing antibodies and cellular immunity. *Front Immunol* 2022; 13: 974364-79. <http://dx.doi.org/10.3389/fimmu.2022.974364> PMID: 36159845
- [22] Feng W, Xiang Y, Wu L, *et al.* Nucleocapsid protein of SARS-CoV-2 is a potential target for developing new generation of vaccine. *J Clin Lab Anal* 2022; 36(6): e24479-88. <http://dx.doi.org/10.1002/jcla.24479> PMID: 35527696
- [23] Primard C, Monchâtre-Leroy E, Del Campo J, *et al.* OVX033, a nucleocapsid-based vaccine candidate, provides broad-spectrum protection against SARS-CoV-2 variants in a hamster challenge model. *Front Immunol* 2023; 14: 1188605-12. <http://dx.doi.org/10.3389/fimmu.2023.1188605> PMID: 37409116

- [24] Dangi T, Class J, Palacio N, Richner JM, Penaloza MacMaster P. Combining spike- and nucleocapsid-based vaccines improves distal control of SARS-CoV-2. *Cell Rep* 2021; 36(10): 109664-74. <http://dx.doi.org/10.1016/j.celrep.2021.109664> PMID: 34450033
- [25] O'Donnell KL, Gourdine T, Fletcher P, Clancy CS, Marzi A. Protection from COVID-19 with a VSV-based vaccine expressing the spike and nucleocapsid proteins. *Front Immunol* 2022; 13: 1025500-9. <http://dx.doi.org/10.3389/fimmu.2022.1025500> PMID: 36353642
- [26] Reguzova A, Müller M, Pagallies F, et al. A multiantigenic Orf virus-based vaccine efficiently protects hamsters and nonhuman primates against SARS-CoV-2. *NPJ Vaccines* 2024; 9(1): 191. <http://dx.doi.org/10.1038/s41541-024-00981-2> PMID: 39414789
- [27] Isakova-Sivak I, Stepanova E, Matyushenko V, et al. Development of a T cell-based COVID-19 vaccine using a live attenuated influenza vaccine viral vector. *Vaccines* 2022; 10(7): 1142-68. <http://dx.doi.org/10.3390/vaccines10071142> PMID: 35891306
- [28] Rak A Y, Donina S A, Isakova-Sivak I N, Rudenko L G. Optimization of purification conditions and study of antigenic properties of recombinant nucleocapsid protein of different SARS-CoV-2 strains. *Med Acad J* 2022; 22: 235-41. <http://dx.doi.org/10.17816/MAJ108599>
- [29] Matyushenko V, Isakova-Sivak I, Kudryavtsev I, et al. Detection of IFN γ -Secreting CD4⁺ and CD8⁺ memory T cells in COVID-19 convalescents after stimulation of peripheral blood mononuclear cells with live SARS-CoV-2. *Viruses* 2021; 13(8): 1490-8. <http://dx.doi.org/10.3390/v13081490> PMID: 34452355
- [30] Liu Z, Chen O, Wall JBJ, et al. Systematic comparison of 2A peptides for cloning multi-genes in a polycistronic vector. *Sci Rep* 2017; 7(1): 2193-201. <http://dx.doi.org/10.1038/s41598-017-02460-2> PMID: 28526819
- [31] Anonymous. Directive 2010/63/EU of the European parliament and of the council of September 22, 2010, on the protection of animals used for scientific purposes. 2010. Available at:<http://eur-lex.europa.eu/legal-content/EN/TXT/?uri=celex%3A32010L0063>
- [32] Yakovlev K S, Mezhenkaya D A, Sivak K V, Rudenko L G, Isakova-Sivak I N. Comparative study of the pathogenicity of SARS-CoV-2 B.1 and B.1.617.2 lineages for syrian hamsters. *Med Acad J* 2022; 22: 125-36. <http://dx.doi.org/10.17816/MAJ109066>
- [33] Matyushenko V, Kotomina T, Kudryavtsev I, et al. Conserved T-cell epitopes of respiratory syncytial virus (RSV) delivered by recombinant live attenuated influenza vaccine viruses efficiently induce RSV-specific lung-localized memory T cells and augment influenza-specific resident memory T-cell responses. *Antiviral Res* 2020; 182: 104864-74. <http://dx.doi.org/10.1016/j.antiviral.2020.104864> PMID: 32585323
- [34] Rak A, Isakova-Sivak I, Rudenko L. Overview of nucleocapsid-targeting vaccines against COVID-19. *Vaccines* 2023; 11(12): 1810-29. <http://dx.doi.org/10.3390/vaccines11121810> PMID: 38140214
- [35] Song Y, Mehl F, Zeichner SL. Vaccine strategies to elicit mucosal immunity. *Vaccines* 2024; 12(2): 191-225. <http://dx.doi.org/10.3390/vaccines12020191> PMID: 38400174
- [36] Thwaites RS, Uruchurtu ASS, Negri VA, et al. Early mucosal events promote distinct mucosal and systemic antibody responses to live attenuated influenza vaccine. *Nat Commun* 2023; 14(1): 8053-66. <http://dx.doi.org/10.1038/s41467-023-43842-7> PMID: 38052824
- [37] Kingstad-Bakke B, Lee W, Chandrasekar SS, et al. Vaccine-induced systemic and mucosal T cell immunity to SARS-CoV-2 viral variants. *Proc Natl Acad Sci USA* 2022; 119(20): e2118312119-130. <http://dx.doi.org/10.1073/pnas.2118312119> PMID: 35561224
- [38] Gallichan WS, Rosenthal KL. Long-lived cytotoxic T lymphocyte memory in mucosal tissues after mucosal but not systemic immunization. *J Exp Med* 1996; 184(5): 1879-90. <http://dx.doi.org/10.1084/jem.184.5.1879> PMID: 8920875
- [39] Zens KD, Chen JK, Farber DL. Vaccine-generated lung tissue-resident memory T cells provide heterosubtypic protection to influenza infection. *JCI Insight* 2016; 1(10): e85832-44. <http://dx.doi.org/10.1172/jci.insight.85832> PMID: 27468427
- [40] Stacey H, Barjesteh N, Mapletoft J, Miller M. "Gnothi Seauton": Leveraging the host response to improve influenza virus vaccine efficacy. *Vaccines* 2018; 6(2): 23-34. <http://dx.doi.org/10.3390/vaccines6020023> PMID: 29649134
- [41] Tong X, Deng Y, Cizmeci D, et al. Distinct functional humoral immune responses are induced after live attenuated and inactivated seasonal influenza vaccination. *J Immunol* 2024; 212(1): 24-34. <http://dx.doi.org/10.4049/jimmunol.2200956> PMID: 37975667
- [42] Netea MG, Joosten LAB. Trained innate immunity: Concept, nomenclature, and future perspectives. *J Allergy Clin Immunol* 2024; 154(5): 1079-84. <http://dx.doi.org/10.1016/j.jaci.2024.09.005> PMID: 39278362
- [43] Pal S, Rafiq Z, Kumari R, et al. Trained innate immunity. *Adv Exp Med Biol* 2025; 1476: 275-96. http://dx.doi.org/10.1007/978-3-031-85340-1_11 PMID: 40622547
- [44] Rudenko L, Yeolekar L, Kiseleva I, Isakova-Sivak I. Development and approval of live attenuated influenza vaccines based on Russian master donor viruses: Process challenges and success stories. *Vaccine* 2016; 34(45): 5436-41. <http://dx.doi.org/10.1016/j.vaccine.2016.08.018> PMID: 27593158
- [45] Isakova-Sivak I, Stepanova E, Mezhenkaya D, et al. Influenza vaccine: progress in a vaccine that elicits a broad immune response. *Expert Rev Vaccines* 2021; 20(9): 1097-112. <http://dx.doi.org/10.1080/14760584.2021.1964961> PMID: 34348561
- [46] Matyushkina D, Shokina V, Tikhonova P, et al. Autoimmune effect of antibodies against the SARS-CoV-2 nucleoprotein. *Viruses* 2022; 14(6): 1141-57. <http://dx.doi.org/10.3390/v14061141> PMID: 35746613
- [47] Nakayama EE, Shioda T. Detrimental effects of anti-nucleocapsid antibodies in sars-cov-2 infection, reinfection, and the post-acute sequelae of COVID-19. *Pathogens* 2024; 13(12): 1109. <http://dx.doi.org/10.3390/pathogens13121109> PMID: 39770368
- [48] Fahoum J, Billan M, Varga JK, et al. Transfer of SARS-CoV-2 nucleocapsid protein to uninfected epithelial cells induces antibody-mediated complement deposition. *Cell Rep* 2025; 44(5): 115512-40. <http://dx.doi.org/10.1016/j.celrep.2025.115512> PMID: 40343796
- [49] Rak A, Donina S, Zabrodskaia Y, Rudenko L, Isakova-Sivak I. Cross-reactivity of SARS-CoV-2 nucleocapsid-binding antibodies and its implication for COVID-19 serology tests. *Viruses* 2022; 14(9): 2041-51. <http://dx.doi.org/10.3390/v14092041> PMID: 36146847
- [50] Thura M, Sng JXE, Ang KH, et al. Targeting intra-viral conserved nucleocapsid (N) proteins as novel vaccines against SARS-CoVs. *Biosci Rep* 2021; 41(9): BSR20211491-505. <http://dx.doi.org/10.1042/BSR20211491> PMID: 34519332
- [51] Del Campo J, Bouley J, Chevandier M, et al. OVX836 heptameric nucleoprotein vaccine generates lung tissue-resident memory CD8⁺ T-Cells for cross-protection against influenza. *Front Immunol* 2021; 12: 678483-95. <http://dx.doi.org/10.3389/fimmu.2021.678483> PMID: 34177921
- [52] Özcengiz E, Keser D, Özcengiz G, Çelik G, Özkul A, İnçer FN. Two formulations of coronavirus disease-19 recombinant subunit vaccine candidate made up of S1 fragment protein P1, S2 fragment protein P2, and nucleocapsid protein elicit strong immunogenicity in mice. *Immun Inflamm Dis* 2022; 10(12): e748-58. <http://dx.doi.org/10.1002/iid3.748> PMID: 36444622
- [53] Nazarian S, Olad G, Abdolhamidi R, et al. Preclinical study of formulated recombinant nucleocapsid protein, the receptor binding domain of the spike protein, and truncated spike (S1) protein as vaccine candidates against COVID-19 in animal models. *Mol Immunol* 2022; 149: 107-18. <http://dx.doi.org/10.1016/j.molimm.2022.06.007> PMID: 35802999

- [54] Yilmaz IC, Ipekoglu EM, Bulbul A, *et al.* Development and preclinical evaluation of virus-like particle vaccine against COVID-19 infection. *Allergy* 2022; 77(1): 258-70. <http://dx.doi.org/10.1111/all.15091> PMID: 34519053
- [55] Gao Y, Wang W, Yang Y, *et al.* Developing next-generation protein-based vaccines using high-affinity glycan ligand-decorated glyconanoparticles. *Adv Sci* 2023; 10(2): 2204598. <http://dx.doi.org/10.1002/advs.202204598> PMID: 36398611
- [56] Matchett WE, Joag V, Stolley JM, *et al.* Cutting edge: Nucleocapsid vaccine elicits spike-independent SARS-CoV-2 protective immunity. *J Immunol* 2021; 207(2): 376-9. <http://dx.doi.org/10.4049/jimmunol.2100421> PMID: 34193597
- [57] Routhu N K, Gangadhara S, Lai L, *et al.* A modified vaccinia ankara vaccine expressing spike and nucleocapsid protects rhesus macaques against SARS-CoV-2 delta infection. *Sci Immunol* 2022; 7(72): eabo0226. <http://dx.doi.org/10.1126/sciimmunol.abo0226> PMID: 35357886 PMID: PMC8995033
- [58] Sergeeva MV, Vasilev K, Romanovskaya-Romanko E, *et al.* Mucosal immunization with an influenza vector carrying SARS-CoV-2 N protein protects naïve mice and prevents disease enhancement in seropositive Th2-Prone Mice. *Vaccines* 2024; 13(1): 15-35. <http://dx.doi.org/10.3390/vaccines13010015> PMID: 39852794